Ultra-wideband Ge-rich silicon germanium integrated Mach-Zehnder interferometer for mid-infrared spectroscopy

Vladyslav Vakarin, Joan Manel Ramírez, Jacopo Frigerio, Andrea Ballabio, Xavier Le Roux, Qiankun Liu, David Bouville, Laurent Vivien, Giovanni Isella, Delphine Marris-Morini

Ultra-wideband Ge-rich silicon germanium integrated Mach Zehnder interferometer for mid infrared spectroscopy

VLADYSLAV VAKARIN,[1,†] JOAN MANEL RAMÍREZ,[1,†] JACOPO FRIGERIO,[2] ANDREA BALLABIO,[2] XAVIER LE ROUX,[1] QIANKUN LIU,[1] DAVID BOUVILLE,[1] LAURENT VIVIEN,[1] GIOVANNI ISELLA[2] AND DELPHINE MARRIS-MORINI[1,*]

[1]*Centre de Nanosciences et de Nanotechnologies (C2N) , Université Paris Sud, CNRS,Université Paris Saclay, 91405 Orsay, France*
[2]*L-NESS, Dipartimento di Fisica, Politecnico di Milano, Polo di Como, Via Anzani 42, 22100 Como, Italy*
**Corresponding author: delphine.morini@u-psud.fr*

Received XX Month XXXX; revised XX Month, XXXX; accepted XX Month XXXX; posted XX Month XXXX (Doc. ID XXXXX); published XX Month XXXX

This work explores the use of Ge-rich $Si_{0.2}Ge_{0.8}$ waveguides on graded $Si_{1-x}Ge_x$ substrate for the demonstration of ultra-wideband photonic integrated circuits in the mid infrared (mid-IR) wavelength range. We designed, fabricated and characterized broadband Mach Zehnder interferometers (MZI) fully covering a range of 3 µm in the mid-IR band. The fabricated devices are operating indistinctly in quasi-TE and quasi-TM polarizations and have an extinction ratio (ER) higher than 10 dB over the entire operating wavelength range. The obtained results are in good correlation with theoretical predictions, while numerical simulations indicate that the device bandwidth can reach one octave with low additional losses. This work paves the way for further realization of mid-IR integrated spectrometers using low-index-contrast $Si_{1-x}Ge_x$ waveguides with high Germanium concentration.

OCIS codes: *(130.0130) Integrated optics; (230.0230) Optical devices; (220.0220) Optical design and fabrication.*

http://dx.doi.org/10.1364/OL.99.099999

Strong and sharp molecular absorption bands of liquids, gases and solids overlap with mid-IR spectral region 2-20 µm. In this context, mid-IR photonic integrated circuits (mid-IR PICs) are very attractive for a growing number of applications such as: medical diagnosis [1], astronomy [2], biosensing [3-4], security [5]. The common principle of operation of these devices is to exploit strong mid-IR absorption present in the substances of interest to detect small compounds of analyte. Concentrations of few parts per billion (ppb) are targeted. Interestingly, mid-IR PICs are also a powerful tool for thermal imaging, astronomy and life detection. Moreover, mid-IR photonic devices can potentially be used for free-space optical communications exploiting mid-IR atmosphere transparency windows: 3-5 µm and 8-13 µm. The use of silicon-based photonics platforms for the mid-IR presents several advantages such as the use of the state-of-the-art mature technology, with large volume fabrication and low production cost, as well as the possibility for component miniaturization which will lead to on-chip-mid-IR sensing platforms. In this context, SOI material platform seems to be a natural choice [6]. However, despite such a promising scenario, the implementation of the devices operating in the mid-IR range is challenging due to SiO_2 absorption beginning around λ=3.6 µm [7]. To tackle this limitation, several approaches have been proposed so far: suspended silicon [8-10], silicon-on-sapphire [11-12], silicon nitride (SiN_x) [13-14]. However, as silicon starts to absorb for wavelengths higher than 8 µm there is a growing interest for new materials to extend the operational wavelength of mid-IR devices. New approaches are currently suggested such as the use of chalcogenide [15-17], Ge-on-Si [18-22], Ge-on-SiN_x [23], low Ge content $Si_{1-x}Ge_x$ alloys [24]. Based on these material platforms low loss rib and strip waveguides have been demonstrated. Ge-on-Si exhibits losses between 0.6 dB/cm to 3 dB/cm for λ=3.8 µm and λ=5.4 µm [20, 22], Ge-on-SiN_x [23] and Si-on-sapphire [11, 12] losses are close to 1-4dB/cm between 4.5 µm and 5.18 µm. Finally, chalcogenide structures pushed the operational wavelength up to 7.7 µm with 2.6 dB/cm [15]. Following these results, numerous building blocks have already been demonstrated using such different platforms including mid-IR wavelength (de)multiplexers based on planar concave gratings (PCGs) [19], arrayed waveguide gratings AWG [18, 25], ring resonators [10, 17], grating couplers [21] or MZIs [20] with 20 dB ER based on Ge on Si waveguides operating between 5.14 µm and 5.4 µm wavelength. Furthermore, low loss multimode interference structures (MMI) with suspended silicon with excess losses below 0.4 dB [8] have been reported. However, it is worth mentioning that all these results have been

performed for a limited wavelength range and until now no broadband (higher than 1 µm wavelength span) operation has been shown in the mid-IR.

Interestingly Ge-rich $Si_{1-x}Ge_x$ alloys are an alternative approach for the exploration of the mid-IR spectral region. Recent Ge-rich $Si_{1-x}Ge_x$ on Si developments showed waveguide losses between 1.5-2 dB/cm at 4.7 µm [26]. Moreover, it has been demonstrated that the use of $Si_{1-x}Ge_x$ alloys offers ultimate control of material bandgap, refractive index properties, light confinement and chromatic dispersion [27]. Additionally, the use of Ge-rich $Si_{1-x}Ge_x$ waveguides potentially allows to address the entire transparency window of Ge i.e. up to λ=15 µm. Furthermore, as Ge has stronger nonlinear parameters than silicon and its TPA vanishes beyond λ=3.2 µm, Ge-rich $Si_{1-x}Ge_x$ alloys are a promising platform for the realization of nonlinear devices in the mid-IR region [27-29]. Finally, this platform is compatible with plasmon-enhanced sensors in the mid-IR based on heavily doped Ge epilayers [30]. In this context we report unique properties of $Si_{0.2}Ge_{0.8}$ waveguides on graded $Si_{1-x}Ge_x$ substrate in term of ultra-wideband operation.

Low energy plasma enhanced chemical vapor deposition (LEPECVD) was used to grow the $Si_{1-x}Ge_x$ material. Ge concentration is increased linearly from 0 to 0.79 along the growth direction over 11 µm thickness with a growth rate of 5-10 nm/s. Then 2 µm thick $Si_{0.2}Ge_{0.8}$ guiding core layer is grown on top of the graded layer. Terminal graded buffer composition is inspected and confirmed by X-ray diffraction. With such approach the lattice parameter is gradually accommodated thus leading to the typical threading dislocation density (TDD) of 3×10^6 cm^{-2} and 3.5 nm rms roughness [31]. Furthermore thanks to the graded buffer layer the optical mode overlaps only with Ge-rich material. The structures were patterned using electron-beam lithography followed by inductively coupled plasma etching (ICP). The etching depth was 4 µm and the waveguide width was 4 µm, as shown in Fig. 1(a), allowing a good confinement for both TE and TM fundamental modes.

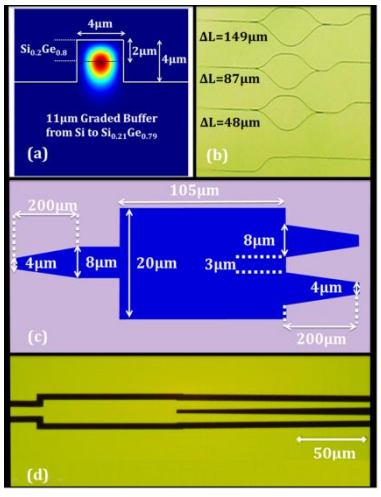

Fig. 1. Fabricated structures: (a) waveguide cross section with the simulated fundamental TE mode, (b) top view of the MZIs, (c) design of the MMI coupler, (d) fabricated MMI, the etched regions appear in black.

Finally, the sidewall roughness was smoothened using hydrogen peroxide solution. The fabricated sample contains asymmetric MZIs with 3 mm long arms and arm length differences of 48 µm, 87 µm and 149 µm and 9.4 mm-long waveguides for transmission comparison (Fig 1(b)). Adiabatic input/output 1.2 mm long tapers were defined for efficient in/out butt coupling to 4 µm thick waveguide. The schematic view of the designed multimode interference structure is depicted in Fig. 1(c) and the corresponding image of the fabricated MMI is shown in Fig. 1(d). Input and output MMI waveguides are tapered over 200 µm length to ensure coupling to the fundamental mode regardless of the operating wavelength.

The transmission measurements were carried out with a mid-IR tunable external Cavity Quantum cascade laser (MIRCAT) operating in pulsed regime. 5 % duty cycle and 100 kHz repetition rate are used. The laser maximum peak intensity was 300 mW, obtained at 6.5 µm wavelength and the exploitable wavelength range was from 5.5 µm to 8.5 µm. The light was coupled in/out of the chip using ZnSe aspheric lenses. A set of mirrors followed by a polarizer are used to collect the light towards an MCT detector. Measurements with 1 nm step were performed using a lock-in amplifier to synchronize the laser pulses with the collected signal. An air drying system was used to purify the air along the light path to minimize the contribution of the environmental absorption. Interestingly, as observed in Fig. 2, the measured transmissions of the 9.4 mm long waveguides are relatively flat on the full wavelength range.

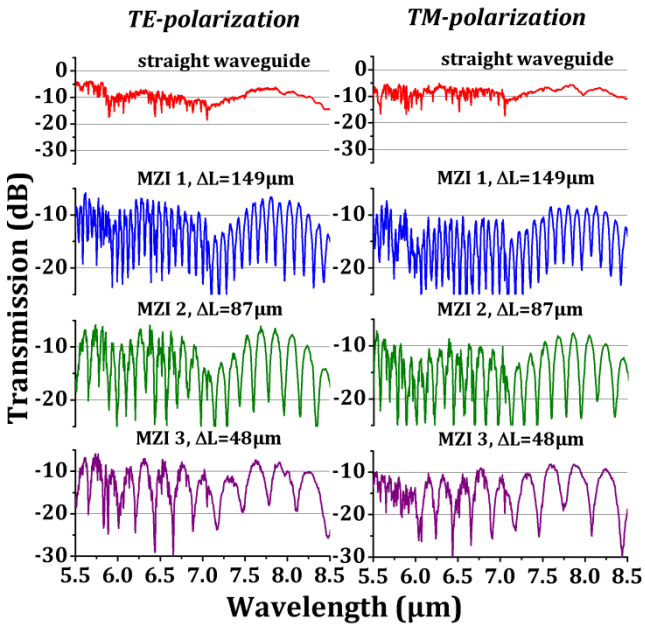

Fig. 2. Transmission measurements in TE and TM polarizations for 9.4 mm-long waveguide and asymmetric MZIs. The reported transmissions include coupling losses in/out of the chip. Red line shows the transmission of the straight waveguide. Blue, green, and purple lines represent the transmission of MZIs with arm difference of: 149 µm, 87 µm and 48 µm respectively. The transmissions are plotted separately to better highlight the spectral features.

The coupling losses were estimated to be around 4 dB/facet and waveguide propagation losses are lower than 5 dB/cm for both polarizations and for the full wavelength range. These values are consistent with previously reported measurements on this type of

waveguides [26]. The larger noise observed at wavelengths between 5.5 μm and 7 μm is observed in all measurements, and is attributed to residual atmosphere peak absorption. The characterizations of the different MZIs in both polarizations are also reported in Fig 2. As it arises from the transmission plots, the devices are ultra-wideband: ER of at least 10 dB between 5.5 μm and 8.5 μm wavelength is obtained both in TE and in TM polarizations. In all the characterized structures we observe the expected decrease of the free spectral range (FSR) with the increase of arm length difference ΔL and the increase of the FSR with the increase of the wavelength. Moreover, no significant degradation of ER or transmission level of the MZI is observed. Additionally when comparing the transmission level of waveguides and MZI, the excess losses of the MZI are always lower than 2 dB in the entire wavelength range from 5.5 μm to 8.5 μm. The unique broadband properties are due to the low vertical confinement and the vertical refractive index gradient in the graded $Si_{1-x}Ge_x$ substrate.

The field intensity profile maps of the MMI coupler are shown in Fig. 3 for different operating wavelengths (λ=5.5 μm, λ=7.5 μm and λ=8.5 μm) and for both polarizations. It is worth mentioning that although such wavelength range was chosen to match the lower and upper limits of our experimental setup, the study at wavelengths lying outside this range (i. e. below 5.5 μm and beyond 8.5 μm) by means of numerical simulations remains interesting to unravel the potentially attainable operation bandwidth of devices.

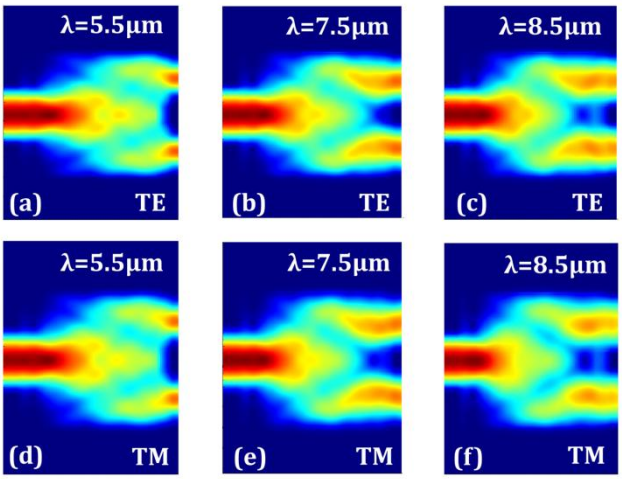

Fig. 3. Electric field intensity profile at λ=5.5 μm, λ=7.5 μm, λ=8.5 μm. TE polarization: (a), (b), (c). TM polarization: (d), (e), (f).

The MMI losses as a function of the wavelength have thus been calculated and the results are reported in Fig. 4 where they are compared with experimental values obtained assuming the excess loss of the MZI comes only from the MMI couplers. A good agreement between theoretical predictions and experimental values is obtained for both polarizations. Several interesting properties of the designed structure arise from the calculation. First and the most remarkable is the device bandwidth. As can be seen from the plot, if we fix 1dB loss limit as a criterion to evaluate the MMI bandwidth (i.e. excess loss of the MZI of 2 dB including both input and output MMI couplers), in TE polarization the device accessible wavelengths are in the range between 5.5 μm and 9 μm i.e. an exploitable bandwidth of 3.5 μm. Moreover, by considering TM polarization, wavelengths between 5.5 μm and 11 μm can be addressed, in other words one octave spanning is accessible with a single device. It is important to point out that another design can be proposed to address the wavelength range from 11 μm to 15 μm to fully cover the Ge transparency window.

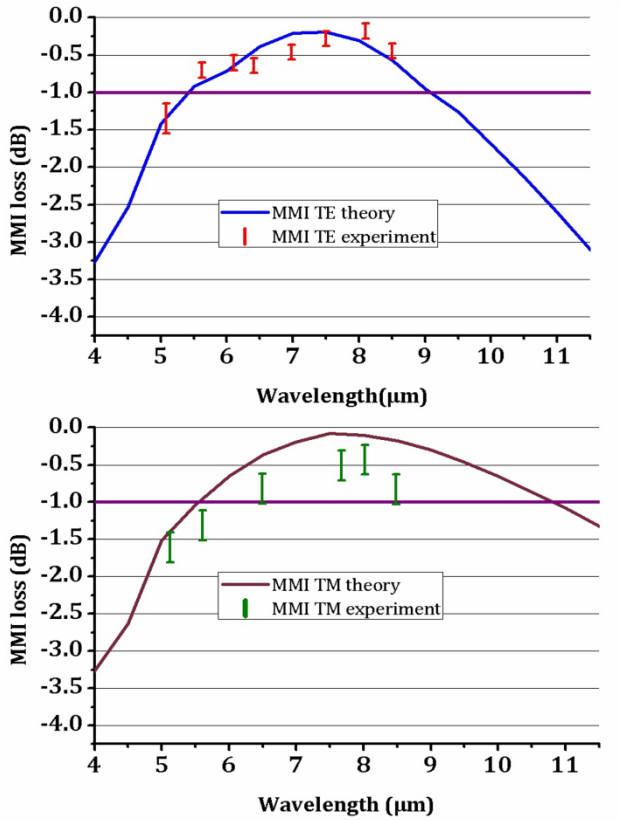

Fig. 4. Experimental and simulated losses for optimized MMI structure in TE and TM polarization. The blue line corresponds to quasi-TE polarization calculation and red bars represent the losses measured on 3 different devices. Similarly for quasi-TM polarization green bars represent the distribution of the measured losses whereas the brown line shows the simulated values. Finally purple line represents 1 dB loss limit that is placed on the plots as eye-guide

In addition, the difference between MMI loss in TE and TM polarization is lower than 0.1 dB for λ ranging from 5 μm to 7 μm. Consequently, according to Fig. 4 it is possible to obtain polarization insensitive MMI operation between 5 μm and 7 μm wavelength and simultaneously maintain MMI losses below 1 dB threshold. The demonstrated broadband MZIs are the basic building block for the realization of broadband mid-IR spectrometer. Indeed, cascaded array of asymmetric MZIs can be used to further build an integrated waveguide Fourier-transform spectrometer [32-33].

In summary, low-loss ultra-wideband asymmetric Mach-Zehnder interferometers have been designed and experimentally demonstrated. The reported structures cover the full range of wavelengths between 5.5 μm and 8.5 μm and until now their operation have only been limited by the setup. Numerical

simulations predict that the bandwidth can be extended up to 9 μm wavelength in TE and 11 μm in TM. These results provide a solid basis for further development of broadband mid-IR spectrometers using Ge-rich $Si_{1-x}Ge_x$ approach that can potentially exploit the whole Ge transparency window, i.e. address wavelengths up to 15 μm.

Funding. French RENATECH Network; European Research Council (ERC) (639107-INsPIRE).

Acknowledgment. Authors acknowledge C2N Nanocenter of the French RENATECH network where the device fabrication was performed. D.M-M. acknowledges support by Institut Universitaire de France.

† Both authors contributed equally to this work

References

1. A. B. Seddon, Int. J. Appl. Glass Sci. **2**, 177 (2011).
2. L. Labadie and O. Wallner, Opt. Express **17**, 1947 (2009).
3. C. Yu, A. Ganjoo, H. Jain, C. G. Pantano, and J. Irudayaraj, Anal. Chem. **78**, 2500 (2006).
4. Z. Han, P. Lin, V. Singh, L. Kimerling, J. Hu, K. Richardson, A. Agarwal, and D. T. H. Tan, Appl. Phys. Lett. **108**, 141106 (2016).
5. Y. C. Chang, P. Wägli, V. Paeder, A. Homsy, L. Hvozdara, P. van der Wal, J. Di Francesco, N.F. de Rooij, and H. P. Herzig, Lab. Chip, **12**, 3020 (2012).
6. G.Z. Mashanovich, M. M. Milošević, M. Nedeljkovic, N. Owens, B. Xiong, E. J. Teo, and Y. Hu, Opt. Express **19**, 7112 (2011).
7. R. Soref, Nat. Photon. **4**, 495 (2010).
8. J. Soler Penades, A. Ortega-Moñux, M. Nedeljkovic, J. G. Wangüemert-Pérez, R. Halir, A. Z. Khokhar, C. Alonso-Ramos, Z. Qu, I. Molina-Fernández, P. Cheben, and G. Z. Mashanovich, Opt. Express **24**, 22908 (2016).
9. A.Vasiliev, A. Malik, M. Muneeb, B. Kuyken, R. Baets, G. Roelkens, ACS Sen. **1**, 1301 (2016).
10. Y. Xia, C. Qiu, X. Zhang, W. Gao, J. Shu, and Q. Xu, Opt. Lett. **38**, 1122 (2013)
11. F. Li, S. D. Jackson, C. Grillet, E.Magi, D. Hudson, S. J. Madden, Y. Moghe, C. O'Brien, A. Read, S. G. Duvall, P. Atanackovic, B. J. Eggleton, and D. J. Moss, Opt. Express **19**, 15212 (2011).
12. T. Baehr-Jones, A. Spott, R. Ilic, A. Spott, B. Penkov, W. Asher, and M.l Hochberg, Opt. Express **18**, 12127 (2010).
13. A. Rahim, E. Ryckeboer, A. Z. Subramanian, S. Clemmen, B. Kuyken, A. Dhakal, A. Raza, A. Hermans, M. Muneeb, S. Dhoore, Y. Li, U. Dave, P. Bienstman, N. Le Thomas, G. Roelkens, D. Van Thourhout, P. Helin, S. Severi, X. Rottenberg, and R. Baets, J. Lightwave Technol. **35**, 639 (2017).
14. P. Tai Lin, V. Singh, L. Kimerling, and A. M. Agarwal, Appl. Phys. Lett. **102**, 251121 (2013).
15. A. Gutierrez-Arroyo, E. Baudet, L. Bodiou, J. Lemaitre, I. Hardy, F. Faijan, B. Bureau, V. Nazabal, and J. Charrier, Opt. Express **24**, 23109 (2016).
16. P. Ma, D.-Y. Choi, Y. Yu, X. Gai, Z. Yang, S. Debbarma, S. Madden, and B. Luther-Davies, Opt. Express **21**, 29927(2013).
17. P. Ma, D.Y. Choi, Y. Yu, Z. Yang, K. Vu, T. Nguyen, A. Mitchell, B. Luther-Davies, and S. Madden, Opt. Express **23**, 19969 (2015)
18. A. Malik, M. Muneeb, S. Pathak, Y. Shimura, J. Van Campenhout, R. Loo,and G. Roelkens, IEEE Photonics Technol. Lett. **25**, 1805 (2013).
19. A.Malik, M. Muneeb, Y. Shimura, J. V. Campenhout, R. Loo, and G. Roelkens, Appl. Phys. Lett. **103**, 161119 (2013)
20. G. Z. Mashanovich, C. J. Mitchell, J. Soler Penades, A. Z. Khokhar, C. G. Littlejohns, W. Cao, Z. Qu, S. Stanković, F. Y. Gardes, T. Ben Masaud, H. M. H. Chong, V. Mittal, G. S. Murugan, J. S. Wilkinson, A. C. Peacock, and M. Nedeljkovic, J. Lightwave Technol. **35**, 624 (2017).
21. C. Alonso-Ramos, M. Nedeljkovic, D. Benedikovic, J.Soler Penadés, C.G. Littlejohns, A. Z. Khokhar, D. Pérez-Galacho, L. Vivien, P. Cheben, and G. Z. Mashanovich, Opt. Lett. **41**, 4324 (2016)
22. A. Malik, M. Muneeb, Y. Shimura, J. V. Campenhout, R. Loo, and G. Roelkens, in Proc. of IEEE Photonics Conference 2013 (IEEE2013) pp. 104105.
23. W. Li, P. Anantha, S. Bao, K. H. Lee, X. Guo, T. Hu, L. Zhang, H. Wang, R. Soref, and C. S. Tan, Appl. Phys. Lett. **109**, 241101 (2016).
24. M. Brun, P. Labeye, G. Grand, J.-M. Hartmann, F. Boulila, M. Carras, and S. Nicoletti, Opt. Express **22**, 508 (2014).
25. P. Barritault, M. Brun, P. Labeye, J.-M. Hartmann, F. Boulila, M. Carras, and S. Nicoletti, Opt. Express **23**, 26168 (2015)
26. J. M. Ramirez, V. Vakarin, C. Gilles, J. Frigerio, A. Ballabio, P. Chaisakul, X. Le Roux, C. Alonso-Ramos, G. Maisons, L. Vivien, M. Carras, G.Isella, and D. Marris-Morini, Opt. Lett. **42**, 105 (2017).
27. J. M. Ramirez, V. Vakarin, J. Frigerio, P. Chaisakul, D. Chrastina, X. Le Roux, A. Ballabio, L. Vivien, G. Isella, and D. Marris-Morini, Opt. Express **25**, 6561 (2017)
28. L. Zhang, A. Agarwal, L. Kimerling, J. Michel, Nanophotonics, **3**, 247 (2013).
29. M. A. Ettabib, L. Xu, A. Bogris, A. Kapsalis, M. Belal, E. Lorent, P. Labeye, S. Nicoletti, K. Hammani, D. Syvridis, D. P. Shepherd, J. H. V. Price, D. J. Richardson, and P. Petropoulos, Opt. Lett. **40**, 4118 (2015).
30. J.Frigerio, A. Ballabio, G.Isella, E.Sakat, G.Pellegrini, P. Biagioni, M.Bolani, E. Napolitani, C. Manganelli, M. Virgilio, A. Grupp, M.P. Fischer, D. Brida, K. Gallacher, D.J. Paul, L. Baldassarre, P. Calvani, V. Giliberti, A. Nucara and M. Ortolani, Phys. Rev. B **94**, 085202 (2016).
31. G. Isella, D. Chrastina, B. Rössner, T. Hackbarth, H. J. Herzog, U. König and H. Von Känel, Solid-State Electron. **48**, 1317 (2004).
32. V. Velasco, P.Cheben, P. J. Bock, A.Delâge, J. H. Schmid, J.Lapointe, S. Janz, M. L. Calvo, D.-X. Xu, M. Florjańczyk, and M. Vachon, Opt. Lett. **38**, 706 (2013).
33. M. Nedeljkovic, A. V. Velasco, A. Z. Khokhar, A. Delâge, P.Cheben and G.Z. Mashanovich, IEEE Photonics. Technol. Lett. **28**, 528 (2016).

FULL REFERENCES

1. A. B. Seddon, "A Prospective for New Mid-Infrared Medical Endoscopy Using Chalcogenide Glasses," Int. J. Appl. Glass Sci. **2**, 177–191(2011).
2. L. Labadie and O. Wallner, "Mid-infrared guided optics: a perspective for astronomical instruments," Opt. Express **17**, 1947-1962 (2009).
3. C. Yu, A. Ganjoo, H. Jain, C. G. Pantano, and J. Irudayaraj, "Mid-IR Biosensor: Detection and Fingerprinting of Pathogens on Gold Island Functionalized Chalcogenide Films," Anal. Chem. **78**, 2500-2506 (2006).
4. Z. Han, P. Lin, V. Singh, L. Kimerling, J. Hu, K. Richardson, A. Agarwal, and D. T. H. Tan, "On-chip mid-infrared gas detection using chalcogenide glass waveguide," Appl. Phys. Lett. **108**, 141106 (2016).
5. Y. C. Chang, P. Wägli, V. Paeder, A. Homsy, L. Hvozdara, P. van der Wal, J. Di Francesco, N.F. de Rooij, and H. P. Herzig, "Cocaine detection by a mid-infrared waveguide integrated with a microfluidic chip," Lab. Chip **12**, 3020 (2012).
6. G.Z. Mashanovich, M. M. Milošević, M. Nedeljkovic, N. Owens, B. Xiong, E. J. Teo, and Y. Hu, "Low loss silicon waveguides for the mid-infrared," Opt. Express **19**, 7112-7119 (2011).
7. R. Soref, "Mid-infrared photonics in silicon and germanium," Nat. Photon. **4**, 495–497 (2010).
8. J. Soler Penades, A. Ortega-Moñux, M. Nedeljkovic, J. G. Wangüemert-Pérez, R. Halir, A. Z. Khokhar, C. Alonso-Ramos, Z. Qu, I. Molina-Fernández, P. Cheben, and G. Z. Mashanovich, "Suspended silicon mid-infrared waveguide devices with subwavelength grating metamaterial cladding," Opt. Express **24**, 22908-22916 (2016).
9. A.Vasiliev, A. Malik, M. Muneeb, B. Kuyken, R. Baets, G. Roelkens, "On-Chip Mid-Infrared Photothermal Spectroscopy using Suspended Silicon-on-Insulator Microring Resonators", ACS Sens. **1**, 1301-1307 (2016).
10. Y. Xia, C. Qiu, X. Zhang, W. Gao, J. Shu, and Q. Xu, "Suspended Si ring resonator for mid-IR application," Opt. Lett. **38**, 1122-1124 (2013)
11. F. Li, S. D. Jackson, C. Grillet, E.Magi, D. Hudson, S. J. Madden, Y. Moghe, C. O'Brien, A. Read, S. G. Duvall, P. Atanackovic, B. J. Eggleton, and D. J. Moss, "Low propagation loss silicon-on-sapphire waveguides for the mid-infrared," Opt. Express **19**, 15212-15220 (2011).
12. T. Baehr-Jones, A. Spott, R. Ilic, A. Spott, B. Penkov, W. Asher, and M.l Hochberg, "Silicon-on-sapphire integrated waveguides for the mid-infrared," Opt. Express **18**, 12127-12135 (2010).
13. A. Rahim, E. Ryckeboer, A. Z. Subramanian, S. Clemmen, B. Kuyken, A. Dhakal, A. Raza, A. Hermans, M. Muneeb, S. Dhoore, Y. Li, U. Dave, P. Bienstman, N. Le Thomas, G. Roelkens, D. Van Thourhout, P. Helin, S. Severi, X. Rottenberg, and R. Baets, "Expanding the Silicon Photonics Portfolio With Silicon Nitride Photonic Integrated Circuits," J. Lightwave Technol. **35**, 639-649 (2017).
14. P. Tai Lin, V. Singh, L. Kimerling, and A. M. Agarwal, "Planar silicon nitride mid-infrared devices," Appl. Phys. Lett. **102**, 251121 (2013).
15. A. Gutierrez-Arroyo, E. Baudet, L. Bodiou, J. Lemaitre, I. Hardy, F. Faijan, B. Bureau, V. Nazabal, and J. Charrier, "Optical characterization at 7.7 µm of an integrated platform based on chalcogenide waveguides for sensing applications in the mid-infrared," Opt. Express **24**, 23109-23117 (2016).
16. P. Ma, D.-Y. Choi, Y. Yu, X. Gai, Z. Yang, S. Debbarma, S. Madden, and B. Luther-Davies, "Low-loss chalcogenide waveguides for chemical sensing in the mid-infrared," Opt. Express **21**, 29927-29937 (2013).
17. P. Ma, D.Y. Choi, Y. Yu, Z. Yang, K. Vu, T. Nguyen, A. Mitchell, B. Luther-Davies, and S. Madden, "High Q factor chalcogenide ring resonators for cavity-enhanced MIR spectroscopic sensing," Opt. Express **23**, 19969-19979 (2015)
18. A. Malik, M. Muneeb, S. Pathak, Y. Shimura, J. Van Campenhout, R. Loo, and G. Roelkens "Germanium-on-silicon mid-infrared arrayed waveguide grating multiplexers," IEEE Photonics Technol. Lett. **25**, 1805-1808, (2013).
19. A.Malik, M. Muneeb, Y. Shimura, J. V. Campenhout, R. Loo, and G. Roelkens, "Germanium-on-silicon planar concave grating wavelength (de)multiplexers in the mid-infrared," Appl. Phys. Lett. **103**, 161119 (2013)
20. G. Z. Mashanovich, C. J. Mitchell, J. Soler Penades, A. Z. Khokhar, C. G. Littlejohns, W. Cao, Z. Qu, S. Stanković, F. Y. Gardes, T. Ben Masaud, H. M. H. Chong, V. Mittal, G. S. Murugan, J. S. Wilkinson, A. C. Peacock, and M. Nedeljkovic, "Germanium Mid-Infrared Photonic Devices," J. Lightwave Technol. **35**, 624-630 (2017).
21. C. Alonso-Ramos, M. Nedeljkovic, D. Benedikovic, J. Soler Penadés, C.G. Littlejohns, A. Z. Khokhar, D. Pérez-Galacho, L. Vivien, P. Cheben, and G. Z. Mashanovich, "Germanium-on-silicon mid-infrared grating couplers with low-reflectivity inverse taper excitation," Opt. Lett. **41**, 4324-4327 (2016)
22. A. Malik, M. Muneeb, Y. Shimura, J. V. Campenhout, R. Loo, and G. Roelkens, "Germanium-on-silicon mid-infrared waveguides and Mach-Zehnder interferometers," in Proc. of IEEE Photonics Conference 2013 (IEEE2013) pp. 104105.
23. W. Li, P. Anantha, S. Bao, K. H. Lee, X. Guo, T. Hu, L. Zhang, H. Wang, R. Soref, and C. S. Tan, "Germanium-on-silicon nitride waveguides for mid-infrared integrated photonics," Appl. Phys. Lett. **109**, 241101 (2016).
24. M. Brun, P. Labeye, G. Grand, J.-M. Hartmann, F. Boulila, M. Carras, and S. Nicoletti, "Low loss SiGe graded index waveguides for mid-IR applications," Opt. Express **22**, 508-518 (2014).
25. P. Barritault, M. Brun, P. Labeye, J.-M. Hartmann, F. Boulila, M. Carras, and S. Nicoletti, "Design, fabrication and characterization of an AWG at 4.5 µm," Opt. Express **23**, 26168-26181 (2015)
26. J. M. Ramirez, V. Vakarin, C. Gilles, J. Frigerio, A. Ballabio, P. Chaisakul, X. Le Roux, C. Alonso-Ramos, G. Maisons, L. Vivien, M. Carras, G.Isella, and D. Marris-Morini, "Low-loss Ge-rich Si0.2Ge0.8 waveguides for mid-infrared photonics," Opt. Lett. **42**, 105-108 (2017).
27. J. M. Ramirez, V. Vakarin, J. Frigerio, P. Chaisakul, D. Chrastina, X. Le Roux, A. Ballabio, L. Vivien, G. Isella, and D. Marris-Morini, "Ge-rich graded-index Si1-xGex waveguides with broadband tight mode confinement and flat anomalous dispersion for nonlinear mid-infrared photonics," Opt. Express **25**, 6561-6567 (2017)
28. L. Zhang, A. Agarwal, L. Kimerling, J. Michel, "Nonlinear Group IV photonics based on silicon and germanium: from near-infrared to mid-infrared", Nanophotonics **3**, 247-268 (2013).
29. M. A. Ettabib, L. Xu, A. Bogris, A. Kapsalis, M. Belal, E. Lorent, P. Labeye, S. Nicoletti, K. Hammani, D. Syvridis, D. P. Shepherd, J. H. V. Price, D. J. Richardson, and P. Petropoulos, "Broadband telecom to mid-infrared supercontinuum generation in a dispersion-engineered silicon germanium waveguide," Opt. Lett. **40**, 4118-4121 (2015).
30. J.Frigerio, A. Ballabio, G.Isella, E.Sakat, G.Pellegrini, P. Biagioni, M.Bolani, E. Napolitani, C. Manganelli, M. Virgilio, A. Grupp, M.P. Fischer, D. Brida, K. Gallacher, D.J. Paul, L. Baldassarre, P. Calvani, V. Giliberti, A. Nucara and M. Ortolani, "Tunability of the dielectric function of heavily doped germanium thin films for mid infrared plasmonics", Phys. Rev. B **94**, 085202.
31. G. Isella, D. Chrastina, B. Rössner, T. Hackbarth, H. J. Herzog, U. König and H. Von Känel, "Low-energy plasma-enhanced chemical vapor deposition for strained Si and Ge heterostructures and devices, " Solid-State Electron. **48**, 1317-1323 (2004).
32. V. Velasco, P.Cheben, P. J. Bock, A.Delâge, J. H. Schmid, J.Lapointe, S. Janz, M. L. Calvo, D.-X. Xu, M. Florjańczyk, and M. Vachon, "High-resolution Fourier-transform spectrometer chip with microphotonic silicon spiral waveguides," Opt. Lett. **38**, 706-708 (2013).
33. M. Nedeljkovic, A. V. Velasco, A. Z. Khokhar, A. Delâge, P.Cheben and G. Z. Mashanovich, "Mid-infrared silicon-on-insulator Fourier-transform spectrometer chip", IEEE Photonics Technol. Lett. **28**, 528-531 (2016).